Transmission time in the reflectionless complex potential*

Yin Cheng(殷 澄)[a], Wang Xian-Ping(王贤平)[b], Shan Ming-Lei(单鸣雷)[a], Han Qing-Bang(韩庆邦)[a]†, and Zhu Chang-Ping(朱昌平)[a]

[a] *Jiangsu Key Laboratory of Power Transmission and Distribution Equipment Technology, Hohai University, Changzhou* 213022, *China*
[b] *School of Physics and Communication Electronics, Jiangxi Normal University, Nanchang* 330022, *China*

(Received 15 January 2014; revised manuscript received 16 April 2014; published online 10 August 2014)

A phase time definition directly obtained from the Schrödinger equation is used to investigate the time delay of a particle scattered by complex reflectionless potential. The artifacts introduced by truncating in the numerical simulation are clarified. The time delay of the transmitted wave packet is found to be equal to the reflection time of the truncated potential. Both time delays are the same as the traversal time in the free space, but shorter than the time taken by a classical particle to pass the same potential.

Keywords: complex reflectionless potentials, transmission time, supersymmetric quantum mechanics

PACS: 03.65.Ca, 03.65.Xp, 03.75.Be **DOI:** 10.1088/1674-1056/23/10/100301

1. Introduction

Unlike the resonance tunneling which usually arises at specific resonant frequencies, the reflectionless concept allows the incident wave packets with broad frequency spectra to fully transmit through a potential profile without any reflection.[1,2] Such reflectionless potentials (RPs) also differ from the widely studied perfectly matched layer, which are applied to the complete absorption of waves in the computation.[3] The research on this remarkable issue has both theoretical and practical significance. First, the well-known reflectionless hierarchy is deeply related to "free space" via the supersymmetric quantum mechanics (SUSY QM) algebra,[4] and intimately connected to the multi-soliton solutions of the Korteweg–de Vries equation.[5,6] Furthermore, these potentials exhibit shape invariance, whose phase contribution of the scattered subwaves is found to be independent of the energy level of the bound states.[7] Secondly, in the fields of plasmonics or metamaterials, the reflectionless potentials may inspire a new design principle for "invisible" material due to the similarity between the Schrödinger equation and the Helmholtz equation. The research on the scattering time issue may provide the theoretical foundation for building new functional devices with a graded refractive index profile.[8]

The complex potential is a subject of active research. For example, the parity–time (PT)-symmetric complex potentials have been widely investigated due to the fact that their corresponding energy spectrum is real.[9] Furthermore, in order to construct a quantum "perfect absorber", much attention has been focused on the propagation characteristics of a wave packet in a complex absorbing potential.[10] The non-hermitian complex potential is receiving more and more attention for its usefulness in the description of chemical reactions, inelastic collisions and "open systems" with injecting sources and absorbing sinks, etc.[11] On the other hand, the time taken by a quantum particle in a scattering event is also a topic full of controversy over the old and famous Hartmen effect.[12] This effect predicts superluminal velocity, which obviously violates relativity but seems to be confirmed by various optical, microwave, and acoustic experiments.[12,13] The present paper addresses the time issue of a wave packet incident on the complex RPs, i.e., the supersymmetric partner potentials of the null potential generated by complex super-potentials, which has not been fully investigated.

To be more specific, there are several interesting issues concerning the scattering process of the complex RPs. First, it is possible to build up new invisible materials inspired by the relevant research. So whether the transmitted wave packet is accelerated or delayed in the RPs, when compared with the free space, should be clarified. Secondly, absorption and enhancement exist and exactly balance each other, which is an important case for the investigation of the validity of the time reversal invariance[13] and the relation between the transmission and reflection time. Finally, truncation must be performed on the potentials for both the numerical simulation and the practical application in metamaterials. The boundary reflections introduced by the truncation and their interference should be carefully examined.

2. Reflection time of complex reflectionless potentials

Both continuous and discrete eigenvalue problems of the supersymmetric partner potentials are related by the SUSY

*Project supported by the Fundamental Research Funds for the Central Universities of Hohai University, China (Grant No. 2012B04114) and the National Natural Science Foundation of China (Grant Nos. 10974044 and 11274091).

†Corresponding author. E-mail: hqb0092@163.com

© 2014 Chinese Physical Society and IOP Publishing Ltd

QM algebra, and these supersymmetric partner potentials will have identical reflection (transmission) probabilities and eigenvalue spectra, except for the ground state. So any supersymmetric partner potential of the null potential (free space) is essentially reflectionless. We begin with two super-potentials

$$W(x)=\begin{cases}-\dfrac{\hbar}{\sqrt{2m}}\dfrac{al}{ax+b\mathrm{i}},\\ -\dfrac{\hbar}{\sqrt{2m}}al\cdot\tanh(ax+b\mathrm{i}),\end{cases} \tag{1}$$

where a and b are real, and l is an integer. Note that the functions in Eq. (1) are complex, which are different from the regular super-potentials. In the paper, the units are chosen such that $\hbar=2m=1$ for simplicity. Based on the supersymmetric quantum mechanics, it is not difficult to construct two hierarchies of complex RPs via Eq. (1), which yields

$$V(x)=\begin{cases}\dfrac{a^2l(l-1)}{(ax+b\mathrm{i})^2},\\ -a^2l(l-1)\sec h^2(ax+b\mathrm{i}),\end{cases}\qquad(l=1,2,3,\ldots). \tag{2}$$

It is easy to see that $l=1$ results in null potential for Eq. (2), so any wave packet with incident energy larger than zero will experience no reflection when scattered by these potentials. In this paper, only the scattering states of these complex RPs are dealt with, and the readers may refer to Ref. [14] for the information about those bound states with particle energy $E<0$. It is slightly different from the real RPs such as the sech^2 potential that the incident wave packet is absorbed in some parts of the complex potential, where the imagined part of the potential is negative, and reconstructed in the rest regions. However, it should be noted that these constructed potentials are PT-invariant since $V(x)=V(-x)^*$ holds for both cases,[10] thus their spectra become purely real. There is no need to verify that the reflection probability of Eq. (2) indeed equals zero. However, when dealing with the time issue, it is necessary to truncate infinity to calculate the time delay. The effect induced by truncation is worth studying for the convenience of computation and practical application.

In this paper we focus on the well established Wigner's phase time or the group delay, which was re-explained as a lifetime rather than a transit time by Winful in an effort to solve the old Hartmen paradox.[12] We consider truncated complex RPs that occupy the region $-L<x<L$, and a particle of definite energy $E>0$ and momentum $\hbar k_0$, incident from the left. The group delay definition for the reflected (transmitted) wave packet is

$$\tau_{\mathrm{r,t}}=\hbar\frac{\partial\phi_{\mathrm{r,t}}}{\partial E}, \tag{3}$$

where ϕ_{r} and ϕ_{t} are the phase shifts of the reflection and transmission coefficient, respectively.

In order to calculate the time delay of the complex RPs, the definition in Eq. (3) must be extended to continuously varying potential first. We begin with the time-independent Schrödinger equation and the equivalent Riccati equation, given respectively by

$$\left[-\frac{\mathrm{d}^2}{\mathrm{d}x^2}+V(x)\right]\psi(x)=E\psi(x), \tag{4}$$

and

$$q'(x)=-\left[q^2(x)+\kappa^2(x)\right], \tag{5}$$

where $q(x)=\psi'(x)/\psi(x)$, $\kappa(x)=\sqrt{2m\left(E-V(x)\right)}/\hbar$ and the derivative with respect to x is denoted by prime. Defining $\varphi(x)=-\arctan\left[q(x)/\kappa(x)\right]$, we have

$$\varphi'(x)=\kappa(x)+\frac{q(x)\kappa'(x)}{q^2(x)+\kappa^2(x)}=\kappa(x)+\Delta\kappa(x), \tag{6}$$

where $\Delta\kappa(x)$ is referred to as the wavenumber of the scattered subwaves[7] and represents the wave nature of the quantum particle. Integrating Eq. (6) over an arbitrary interval $a<x<b$ yields

$$\int_a^b\mathrm{d}\varphi(x)=n\pi+\varphi(b)-\varphi(a), \tag{7}$$

where n is the number of nodes of $\kappa(x)\psi(x)$ in the interval. It is clear that Eq. (7) is directly derived from the Schrödinger equation without making any approximation; we turn Eq. (7) into the exact expression of the reflection coefficient. Note that κ is complex for a complex potential, and we do not follow the usual procedure of dividing the coordinate into classically allowed and forbidden regions, since the distinction between them is blurred. Instead, the wave function at any coordinate x_0 can be mathematically expressed as the superposition of incident and reflected waves via

$$\psi(x_0)=C\left[\mathrm{e}^{\mathrm{i}\kappa(x-x_0)}+r(x_0)\,\mathrm{e}^{-\mathrm{i}\kappa(x-x_0)}\right], \tag{8}$$

where $r(x_0)$ denotes the reflection coefficient, which can be defined mathematically in all the regions by recasting the wave function into the form of Eq. (8). Furthermore, approaching to the limit of $x\to+\infty$, $r(x_0)$ should be zero, since there will be no leftward traveling or exponential increasing component at infinity. From Eq. (8), it follows that

$$r(x)=\frac{\kappa(x)+\mathrm{i}q(x)}{\kappa(x)-iq(x)}=\exp\left[-\mathrm{i}2\varphi(x)\right]. \tag{9}$$

Combining Eqs. (7) and (9), one obtains the relation of the reflection coefficient at two different coordinates a and b as

$$r(a)=r(b)\exp\left[2\mathrm{i}\int_a^b(\kappa+\Delta\kappa)\mathrm{d}x\right]. \tag{10}$$

For the truncated complex RPs considered in this paper, equation (10) becomes

$$r(-L)=r(L)\exp\left[2\mathrm{i}\int_{-L}^{L}(\kappa+\Delta\kappa)\mathrm{d}x\right], \tag{11}$$

with

$$r(L) = \frac{\kappa(L) - k_0}{\kappa(L) + k_0}.$$

Applying Eq. (3) to Eq. (11), the group delay for the reflected wave packet is directly derived from the Schrödinger equation and can be divided into two parts. The first part determined by the momentum $p = \hbar\kappa$ is

$$\begin{aligned}\tau_{\rm cl}\Big|_{-L}^{L} &= 2\,{\rm Re}\left(\int_{-L}^{L}\frac{\partial(\hbar\kappa)}{\partial E}{\rm d}x\right)\\ &= 2\,{\rm Re}\left(\int_{-L}^{L}\frac{1}{v_{\rm cl}(x)}{\rm d}x\right),\end{aligned} \tag{12}$$

where $v_{\rm cl}(x)$ is the velocity of a particle and obeys the laws of classical mechanics in the same potential. So equation (12) coincides with the classical reflection time of the particle reflected at the right truncated point and appears at the left boundary. The difference between the classical reflection time $\tau_{\rm cl}$ and its quantum counterpart $\tau_{\rm r}$ is given by the second part

$$\Delta\tau\Big|_{-L}^{L} = 2\hbar\,{\rm Re}\left(\frac{\partial}{\partial E}\int_{-L}^{L}\Delta\kappa{\rm d}x\right), \tag{13}$$

which is completely specified by the wavenumber of the scattered subwaves. On the other hand, the transmission coefficient directly obtained from the wave equation has not been obtained yet, so we use the transfer matrix method[15,16] through the numerical simulation to obtain the transmission coefficient and the transmission time.

3. Truncation-induced nonzero reflection probability

Theoretically, both complex RPs in Eq. (2) yield non-resonant perfect unitary transmission for incident waves with broadband frequency spectra according to SUSY QM. Whenever a computation of electromagnetic scattering is performed by a volume discretization procedure, the truncation is necessary. So we need to truncate infinity to simulate the scattering time. As a result, the corresponding perturbation on reflection probability must be evaluated first. The original potential is reflectionless and any reflection occurs in the truncated potential and results from the interference between the reflections at the boundaries, so these potentials provide us with the perfect opportunity to detect the perturbation of the performed truncation. It should also be noted that in this paper, the wavefunction is calculated numerically by the transfer matrix method, whose accuracy depends on the layer segmentation of the potential, and this algorithm can be applied to the general cases. On the other hand, analytical solutions[14,17] for the reflectionless potentials considered in this paper can be derived and substituted into the reflection time expressions directly. We consider the complex RP $V_{\rm RP}(x)$ with reciprocal superpotential and truncated at $\pm L = \pm 8$, its reflection probability for parameters $a = 1$, $b = 1$, and $l = 2$ is shown in Fig. 1(a). It is clear that the reflection probability approaches to unity at the limit $E \to 0$, and does not decrease monotonically as the particle energy increases. In Fig. 1(b), we show the calculated reflection probability of a rectangular potential well with the same length for comparison, whose well depth equals the potential strengths of the truncated RPs at the truncated points $t_{\rm l}$ and $t_{\rm r}$, i.e.,

$$V(x) = V_{\rm RP}(t_{\rm l}) = V_{\rm RP}(t_{\rm r}), \quad (t_{\rm l} < x < t_{\rm r}). \tag{14}$$

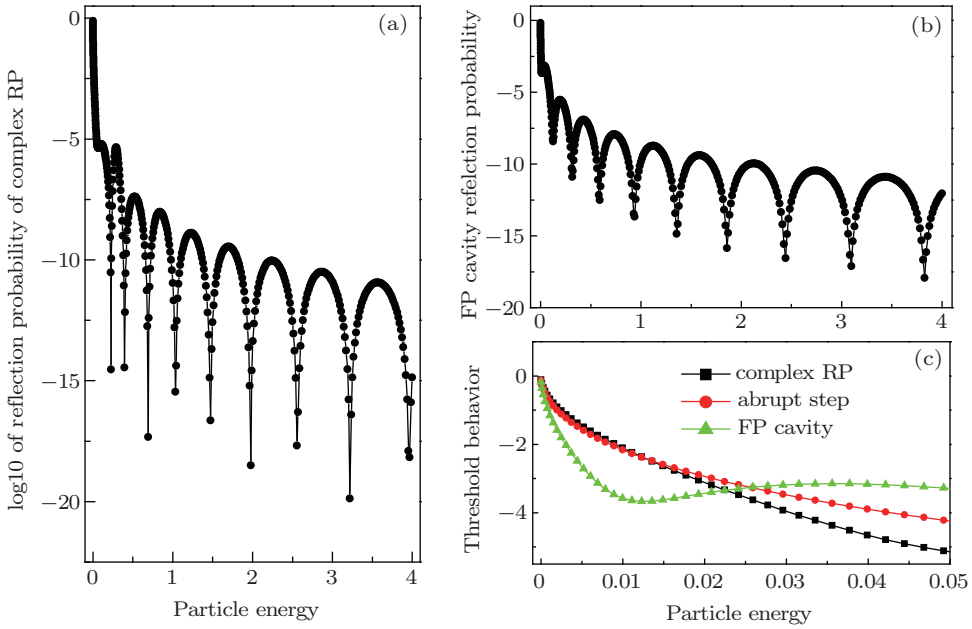


Fig. 1. (color online) (a) Reflection probability of a truncated complex RP $V_{\rm RP}(x)$ as a function of energy, (b) the reflection probability of the rectangular well (Fabry–Perot (FP) cavity), and (c) the threshold behaviors of the reflection probabilities of the truncated RP, the FP cavity and the abrupt step. Note that a logarithmic scale is chosen for the y axis in Fig. 1.

The resonance in Fig. 1(b) can be understood as an FP-like resonance caused by the reflection at the entrance surface and the exit surface, so we refer to this potential as the FP cavity. In Fig. 1(c), the threshold behavior of the complex RP is compared with that of the FP cavity (14) and an abrupt step at the left truncated point is given by

$$V(x) = V_{\mathrm{RP}}(t_1), \quad (t_1 < x). \tag{15}$$

Potential (14) focuses on the reflection at the left truncated point only, which is crucially near the zero energy limit. A schematic diagram of the three potentials are plotted in Fig. 2, where only the real part of the complex RP is illustrated.

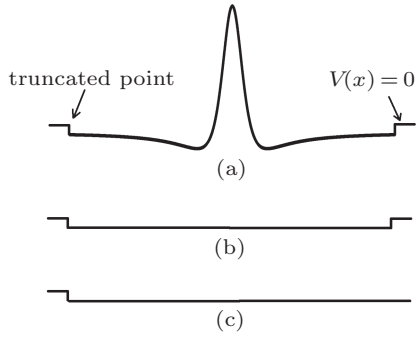


Fig. 2. (a) Real part of the truncated complex RP, the rectangular potential well (FP cavity) (Eq. (14)) and the abrupt step at the left truncated point (Eq. (15)).

The original complex RPs are reflectionless, and the truncated points reflect the wave and lead to nonzero reflection spectrum. Comparing Fig. 1(a) with Fig. 1(b), it is obvious that the resonance-like behavior in the reflection probability of the truncated RP results from the interference between the multiple reflections at the two truncated points. However, as can be seen in Fig. 1(c), the near threshold of the truncated RP is determined by the reflection at the left truncated point only. Similar conclusions can also be drawn when the truncated complex sech-squared potential is simulated. In order to minimize the effect of truncation on the scattering time simulation, the complex RPs should be truncated at larger x.

4. Transmission time and the scattered sub-waves

The incident wave packets scattered by the complex RPs and the null potential have the same reflection spectra, but do they experience the same time delays? Since all the potentials extend to infinity, we need to truncate both potentials for a numerical comparison. Importantly, for the truncated complex RPs, numerical simulation confirms that the transmission time calculated by the transfer matrix method is equal to the reflection time calculated from Eqs. (12) and (13). So despite the fact that the potential is complex, the time reversal invariance may still hold for the complex RPs. In the rest of the present paper, both the transmission time and the reflection time of the complex RPs are referred to as time delay. The transmission time through the free space (null potential) of the same length is simply

$$t_{\mathrm{null}} = \frac{2Lm}{\hbar k_0}. \tag{16}$$

Furthermore, it is also interesting to compare this with the time taken by a classical particle traveling through the same potential

$$t_{\mathrm{cl}} = \mathrm{Re}\int_{-L}^{L} \frac{m}{\hbar\kappa(x)}\,\mathrm{d}x. \tag{17}$$

The value obtained from Eq. (17) is just half that from Eq. (12). Figure 3 plots the time delay of the complex potential $\tau_{\mathrm{cl}} + \Delta\tau$, t_{cl} for the complex RP $V_{\mathrm{RP}}(x)$ with $a = 1$, $b = 1$, $l = 2$, and t_{null} for the null potential. All these potentials are truncated at $\pm L = \pm 50$.

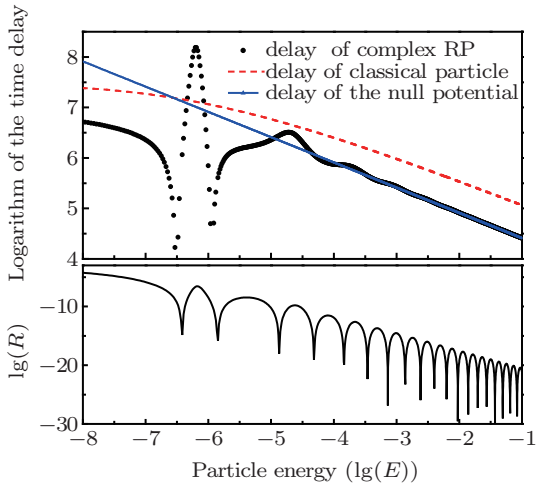


Fig. 3. (color online) Calculated time delay $\tau_{\mathrm{cl}} + \Delta\tau$ of the complex RP locates between $[-50,\ 50]$, the traversal time t_{cl} of the classical particle through the same potential and the transmission time t_{null} through the null potential (free space). For comparison, the reflection probability of the truncated RP is also plotted.

We still focus on the near threshold behavior of the time delay of the truncated complex RP, which is obviously perturbed by the truncation. But at higher energy such as $E > 0.001$, the perturbation can be ignored and the time delay obviously coincides with the transmission time in the free space, and the classical particle takes the longest time to transmit through the same complex potential. As the particle energy decreases, i.e., $10^{-7} < E < 10^{-3}$, the perturbation becomes apparent and the time delay has a similar pattern to the reflection probability. However, at the threshold, the reflection increases exponentially due to the fact that the particle energy is comparable to the abrupt variation of the potential's real part at the left truncated point. Since most of the particles are reflected before entering into the potential region, the phase time of the quantum particle $\tau_{\mathrm{cl}} + \Delta\tau$ is saturated at this limit. As pointed out by Winful,[12] the phase time definition cannot be related to the superluminal velocity. We also need to point out

that the saturation of the classical particle t_{cl} delay time at the zero energy limit can be attributed to the occurrence of the barrier region. The same complex RP is simulated again with a longer truncation length and the results are plotted in Fig. 4.

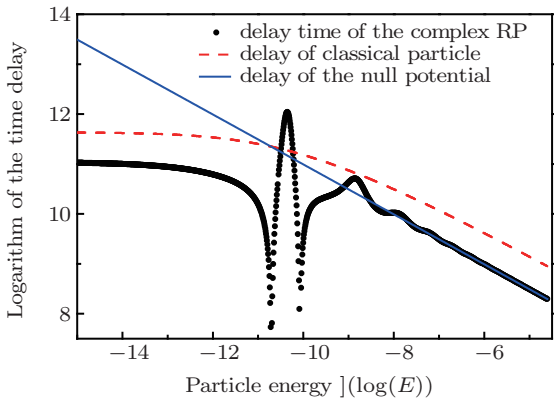


Fig. 4. (color online) Time delay of the quantum particle and the classical particle in the complex RP located between $[-400,\ 400]$. For comparison, the transmission time through the free space is also given.

The truncation length of the potential simulated in Fig. 4 is much longer than that in Fig. 3, so it is closer to the case where the complex RP extends to infinity. Comparing Fig. 3 with Fig. 4, conclusions can be drawn that the time delay of the complex RPs without truncation will be equal to the transmission time of the free space, and smaller than the transmission time of a classical particle. This conclusion is of great importance, since it allows wave packets to completely transmit through the complex RPs with the same time delay as in the free space. As a result, novel metamaterials with potential application such as invisibility can receive much attention. Considering Eqs. (12) and (16), the subwaves-induced time delay $\Delta\tau$ of the complex RP that extends to infinity can be easily calculated from

$$\Delta\tau(k_0) = \int_{-\infty}^{\infty} \frac{m}{\hbar}\left(\frac{1}{k_0} - \frac{2}{\kappa(x)}\right) \mathrm{d}x. \tag{18}$$

5. Conclusions

In this paper, we investigated the time delay of the complex supersymmetric partner potentials of the free space. A reflection time directly derived from the Schrödinger equation and the phase time definition are discussed. The numerical simulations demonstrate that both the transmission time and the reflection time of the complex RPs are equal to the transmission time in the free space. It is also clear that the wave packet is accelerated when compared with a classical particle in the same potential.

Acknowledgment

The authors want to thank Prof. Tan at Hohai University for helpful discussion.

References

[1] Sukhorukov A 2010 *Opt. Lett.* **35** 989
[2] Correa F, Jakubský V and Plyushchay M 2009 *Ann. Phys.* **324** 1078
[3] Berenger J 1994 *J. Comput. Phys.* **114** 185
[4] Cooper F, Khare A and Sukhatme U 1995 *Phys. Rep.* **251** 267
[5] Koller A and Olshanii M 2011 *Phys. Rev. E* **84** 066601
[6] Park C 2011 *Phys. Lett. A* **375** 3348
[7] Yin C, Cao Z and Shen Q 2010 *Ann. Phys.* **325** 528
[8] Szameit A, Dreisow F, Heinrich M, Nolte S and Sukhorukov A 2011 *Phys. Rev. Lett.* **106** 193903
[9] Ahmed Z 2001 *Phys. Lett. A* **282** 343
[10] Muga J, Palao J, Navarro B and Egusquiza I 2004 *Phys. Rep.* **395** 357
[11] Pandya S, Vaishnav B and Joshipura K 2012 *Chin. Phys. B* **21** 093402
[12] Winful H 2006 *Phys. Rep.* **436** 1
[13] Steinberg A and Chiao R 1994 *Phys. Rev. A* **49** 3283
[14] Zhou G 1993 *Acta Phys. Sin.* **42** 173 (in Chinese)
[15] Yuan W, Yin C, Wang X and Cao Z 2010 *Chin. Phys. B* **19** 093402
[16] Yin. C, Wu. Z, Wang X, Sun J and Cao Z 2010 *Chin. Phys. B* **19** 117305
[17] Hai W, Rong S and Zhu Q 2008 *Phys. Rev. E* **78** 066214